Food Chemistry: X 22 (2024) 101347

Contents lists available at ScienceDirect

Food Chemistry: X

journal homepage: www.sciencedirect.com/journal/food-chemistry-x

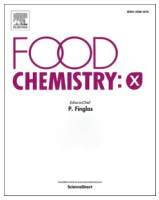

Relationship between microstructure formation and *in vitro* starch digestibility in baked gluten-starch matrices

José D. Torres [a,c], Verónica Dueik [b], Ingrid Contardo [d,e], David Carré [b], Pedro Bouchon [a,f,*]

[a] Department of Chemical and Bioprocess Engineering, Pontificia Universidad Católica de Chile, PO Box 306, Santiago 6904411, Chile
[b] Comercial e Industrial SOLUTEC Ltda, Almirante Churruca 3130, Santiago 8370653, Chile
[c] School of Agroindustrial Engineering, Universidad del Sinú Cartagena, Sede Plaza Colón, Avenida El Bosque, Transversal 54 N° 30-729, Cartagena 130014, Colombia
[d] Biopolymer Research and Engineering Lab (BiopREL), School of Nutrition and Dietetics, Faculty of Medicine, Universidad de los Andes, Monseñor Álvaro del Portillo 12.455, Chile
[e] Centre for Biomedical Research and Innovation (CIIB), Universidad de los Andes, Monseñor Álvaro del Portillo 12.455, Las Condes, Chile
[f] Centro de Investigación en Nanotecnología y Materiales Avanzados (CIEN-UC), Pontificia Universidad Católica de Chile, PO Box 306, Santiago 6904411, Chile

ARTICLE INFO

Chemical compounds studied in this article:
Inulin (PubChem CID: 132932783)
Polydextrose (PubChem CID: 71306906)
Benzoic acid (PubChem CID: 243)
Hydrochloric acid (PubChem CID: 313)
Potassium hydroxide (PubChem CID: 14797)
Sodium acetate 3-Hydrate (PubChem CID: 23665404)
Acetic acid (PubChem CID 176)
Pepsin (PubChem CID: 17397483)
Pancreatin (PubChem SID 7,980,246)
Invertase (PubChem SID 348266890)

Keywords:
Inulin
Polydextrose
Baking
Gelatinization
X-ray micro-computed tomography
Starch digestibility

ABSTRACT

Increased prevalence of diabetes prompts the development of foods with reduced starch digestibility. This study analyzed the impact of adding soluble dietary fiber (inulin-IN; polydextrose-PD) to baked gluten-starch matrices (7.5–13%) on microstructure formation and *in vitro* starch digestibility. IN and PD enhanced water-holding capacity, the hardness of baked matrices, and lowered water activity in the formulated matrices, potentially explaining the reduced starch gelatinization degree as IN or PD concentration increased. A maximum gelatinization decrease (26%) occurred in formulations with 13% IN. Micro-CT analysis showed a reduction in total and open porosity, which, along with the lower gelatinization degree, may account for the reduced *in vitro* starch digestibility. Samples with 13% IN exhibited a significantly lower rapidly available glucose fraction (8.56 g/100 g) and higher unavailable glucose fraction (87.76 g/100 g) compared to the control (34.85 g/100 g and 47.59 g/100 g, respectively). These findings suggest the potential for developing healthier, starch-rich baked foods with a reduced glycemic impact.

1. Introduction

Diabetes is one of the most common diet-related chronic diseases associated with high blood glucose levels and is the cause of severe health problems (Chen et al., 2024). The global population with diabetes reached 475 million in 2020, and it is expected to rise to 700 million by 2045, presenting a significant economic burden on healthcare systems (Sun et al., 2022). Furthermore, the COVID-19 pandemic has presented unprecedented challenges for individuals with diabetes, as they face an increased risk of infection and mortality (Sharma et al., 2022). According to Lim, Bae, Kwon, and Nauck (2021), there is a strong association between diabetes and COVID-19, with a 30% increase in risk. Consequently, it is relevant to develop starchy food products that can aid in managing this pathology.

Starchy foods, such as fried, baked, or extruded products, are primarily composed of starch, an essential carbohydrate that serves as a relevant energy source in the human diet (Contardo, James, & Bouchon, 2020). These foods are widely commercialized due to their affordability and convenience for immediate consumption (Bello-Pérez, Flores-Silva, Agama-Acevedo, & Tovar, 2020). However, a high intake of starch-rich foods has been associated with increased postprandial blood glucose levels (Zhang, Sun, & Ai, 2022).

Starch transforms during thermal processing (*e.g.,* gelatinization), making it digestible for humans (Zhou, Ye, Lei, Zhou, & Zhao, 2022). It

* Corresponding author at: Department of Chemical and Bioprocess Engineering, Pontificia Universidad Católica de Chile, PO Box 306, Santiago 6904411, Chile.
E-mail address: pbouchon@uc.cl (P. Bouchon).

https://doi.org/10.1016/j.fochx.2024.101347
Received 12 January 2024; Received in revised form 18 March 2024; Accepted 31 March 2024
Available online 3 April 2024

is well known that starch digestion initiates in the mouth, and glucose absorption occurs in the small intestine. Based on the rate and extent of enzymatic digestion, starch can be classified into three glucose fractions: *rapidly available glucose* (RAG), digested in the first 20 min; *slowly available glucose* (SAG), digested between 20 and 120 min; and *unavailable glucose* (UG), which remains unabsorbed after 120 min (Contardo, Parada, Leiva, & Bouchon, 2016). It is crucial to control the intake of RAG-rich foods as these could induce hyperglycemia. Conversely, foods rich in SAG and UG offer potential health benefits, including stable glucose metabolism. Consequently, research has been performed to increase SAG and UG content in starchy foods without compromising their sensory attributes (Bello-Pérez & Flores-Silva, 2023). Multiple factors, such as botanical source, thermal processing, and interaction with phytochemicals and biomolecules, can affect starch digestibility (Toutounji et al., 2019). There is a growing scientific interest in utilizing functional ingredients to regulate starch digestion rates and produce food products with a reduced glycemic impact without compromising their nutritional properties (Yang, Zhang, Wu, & Ouyang, 2023).

Dietary fibers (DF) are a group of non-digestible and heterogeneous biopolymers used as functional compounds in starchy foods. These compounds are classified as insoluble (IDF) and soluble (SDF) in water (Dueik, Sobukola, & Bouchon, 2014). The intake of SDF has been associated with prolonged gastric emptying, increased beneficial microbiota, lowered cholesterol, and decreased postprandial glucose levels (Zhou et al., 2021). Among the SDFs used in starchy foods are inulin (IN) and polydextrose (PD). IN is a fructan linked by β-(2 → 1) fructosyl-fructose glycosidic bonds, whereas PD is a synthetic glucose-derived compound that contains glycosidic α and β-(1 → 6) bonds. Both are bulking agents, sweeteners, thickeners, texture modifiers, and food stabilizers (Torres, Dueik, Carré, & Bouchon, 2019).

The possible reduction of starch digestibility in the presence of IN and PD has been linked to the viscosity developed during intestinal digestion, changes in starch microstructure, and modification of starch gelatinization (Goff, Repin, Fabek, El Khoury, & Gidley, 2018). The high viscosity is determined by the ability of IN and PD to thicken when mixed with water molecules due to physical entanglements between the functional groups (Zhang et al., 2022). Accordingly, IN and PD could limit nutrient movements in the small intestine and inhibit glucose absorption. Besides, the high water-binding capacity of IN and PD could reduce water activity, hindering gelatinization (Yang et al., 2023; Zhang et al., 2021). In a preliminary study, Torres et al. (2019) reported a reduction of starch digestibility in starchy matrices with IN and PD. However, they did not analyze the link between product microstructure, starch gelatinization, and SDF concentration, which could provide valuable information to understand the relationship with starch digestibility better.

Microstructure plays an essential role in determining the physical properties of foods. Therefore, understanding starch microstructural changes during digestion would help in designing starchy foods with suitable textural properties and a low glycemic index (Aguilera, 2022). Studies on starch digestion and food microstructure have focused on obtaining the released glucose. In contrast, the inhibition of digestive enzymes in a simulated gastrointestinal tract is often studied when model starchy matrices have lost their structural integrity (Tian et al., 2019). This highlights the significance of food structures and their breakdown in starch digestibility and subsequent glycemic response (Bello-Pérez et al., 2020; Bello-Pérez & Flores-Silva, 2023; Contardo et al., 2020). Nevertheless, studies on how IN and PD modify the microstructure of starchy foods and affect their digestibility still need to be completed. Consequently, understanding the relevant underlying mechanisms is crucial (Zheng et al., 2021).

Traditionally, microstructural studies involve different microscopy techniques (*e.g.,* scanning electron microscopy, SEM; confocal laser scanning microscopy, CLSM; light microscopy, LM), which may present some disadvantages, such as sample staining and sectioning (LM) or sample dehydration, physical sectioning, and coating (SEM), to name a few (Schoeman, Williams, du Plessis, & Manley, 2016). Although CLSM may overcome the drawbacks of physical sectioning through laser optical sectioning, the observation volume is limited, and adding fluorophores is frequently needed (Contardo & Bouchon, 2018). Some of these limitations may be addressed through X-ray micro-computed tomography (micro-CT), primarily used to analyze the inner structure of a porous sample non-invasively and with high resolution. The foundation of the micro-CT technique lies in the variation of X-ray attenuation intensity within the scanned material, demonstrated through the reconstructed grayscale of every micro-CT image voxel (Van Dyck et al., 2014). This allows for the quantitative characterization of 3D dimensional volumes, enhancing our understanding of food microstructure (Olakanmi, Karunakaran, & Jayas, 2023). Accordingly, the microstructures of starchy foods, such as wheat bread (Chen et al., 2021), rotary-moulded biscuits (Molina, Vaz, Leiva, & Bouchon, 2021), fried starch-gluten matrices (Contardo et al., 2020), rice-flour pellets (Zambrano, Contardo, Moreno, & Bouchon, 2022), and third generation extruded rice snacks (Zambrano, Mariotti-Celis, & Bouchon, 2024) have been successfully characterized using micro-CT. Consequently, this research aimed to analyze the effect of IN and PD addition on microstructure formation in baked gluten-starch matrices and its relationship to starch gelatinization and *in vitro* starch digestibility.

2. Materials and methods

2.1. Reagents

The main ingredients were vital wheat gluten (G) and native starch (S) with a moisture content of 5.9 ± 0.5% and 12.3 ± 0.7% (wet basis, wb), respectively, provided by Roquette® in France. The soluble dietary fibers (SDFs) used included inulin (IN, Fibruline® I, ≥ 90% purity; 4.3% moisture, wb), purchased from Cosucra Groupe Warcoing S.A., Belgium, and polydextrose (PD, Fiber® C, ≥ 95% purity; 1.5% moisture, wb) acquired from Baolingbao Biology, China. Distilled water was obtained from Sumilab S.A., Chile.

Pepsin-7000 from porcine gastric mucosa powder (CAS: 9001-75-6; ≥ 250 U/mg), amyloglucosidase-A7095 from *Aspergillus niger* (CAS: 9001-62-1; ≥ 260 U/mL), and pancreatin-7545 from porcine pancreas (CAS: 8049-47-6; 8 × USP specifications) were used. Other ingredients, such as guar gum (No-G4129), reactive benzoic acid (No. 242381 ≥ 99.5%), acetic acid 1 M (No. 537020 ≥ 99.9%), hydrochloric acid (No. 433160, Sigma-Aldrich, St Louis, MO, USA.), invertase-390203D (CAS 9001-57-4; International Ltd., Poole, UK.), potassium hydroxide in lentils (No. PO-1300), and sodium acetate 3-Hydrate (No. SO-1400, Winkler Ltda. Santiago, Chile), were used for *in vitro* starch digestibility assays.

2.2. Sample preparation and processing

Laminated doughs were prepared with G and S at a dry basis (db) ratio of 12% and 88%, respectively. All samples were developed to ensure the same moisture content (40% wb). The added water was adjusted, considering the initial water content of each ingredient. Other laminated doughs were prepared by replacing starch with IN or PD, adding 7.5 or 13 g/100 g (*i.e.,* IN7.5%, IN13%, PD7.5%, and PD13% throughout the manuscript, as shown in Table 1). Based on the literature review and preliminary assays, the ingredients and amounts to obtain an adequate dough structure were chosen (Dueik et al., 2014). The G level was constant to guarantee the dough's sheetability without incorporating additional ingredients. The SDF concentration was fixed based on preliminary starch digestion analyses, revealing that amounts lower than 7.5% of SDFs did not significantly modify starch digestibility. In contrast, levels higher than 13% impaired dough formation.

Dry ingredients were mixed for 2 min using a 5K5SS mixer (KitchenAid, St. Joseph, MI, USA) equipped with a K5AB flat beater. Half the water was added at 15 °C while mixing at 40 rpm for 1 min.

Table 1
The composition of the different starchy formulations.

Ingredients										
Product code	G (gluten)		S (starch)		SDF (soluble dietary fibers)				Moisture content (wet basis)	
					IN (inulin)		PD (polydextrose)			
	(%)	(g/100 g)	(%)	(g/100 g)	(%)	(g/100 g)	(%)	(g/100 g)	(%)	(g/100 g)
Control	12	21.1	88.0	159	–	–	–	–	40	110.3
IN7.5%	12	21.1	80.5	148	7.5	10.9	–	–	40	110.9
IN13%	12	21.1	75	140	13.0	18.3	–	–	40	113.6
PD7.5%	12	21.1	80.5	148	–	–	7.5	10.6	40	110.6
PD13%	12	21.1	75	140	–	–	13.0	18.6	40	113.1

Subsequently, the remaining amount was added at 90 °C while mixing for 3 min (Contardo et al., 2016). The dough was then stored inside a plastic film for one hour to avoid moisture loss. The doughs were sheeted using an LSB516 dough sheeter (Doyon, Saint-Côme-Linière, Quebec, Canada) until a final thickness of 5 mm was achieved. The sheeted dough was cut into squares (3 × 3 cm^2), ensuring a constant weight (2.7 ± 0.2 g). The baking process was carried out in an electric forced convection oven (model self-cooking center®, Rational AG., Germany) with 0% relative humidity at 170 °C, up to a moisture content of 6.0 ± 1.0% (db) in all samples. Baked gluten-starch matrices were incorporated in self-closing polypropylene bags with minimal headspace and then stored under controlled temperature and relative humidity conditions for up to 2 h before physicochemical analysis.

2.3. Moisture changes

2.3.1. Moisture content

Moisture content was analyzed according to AOAC (1995). The samples were dried to a constant weight at 105 °C for 24 h in a forced-air oven (LDO-080F, Labtech Co., Ltd., Namyangju, Korea).

2.3.2. Water activity analysis

A portable instrument (Novasina™ ms1-set aw, Lachen, Switzerland) was used to measure the water activity (Aw) of the different starchy formulations at 25 °C. The device was calibrated using saturated salt solutions of known relative humidity, namely, 11.3, 32.8, 52.9, 75.3, and 90.1%. After the calibration, 5 g of crushed sample were placed inside the measuring chamber. The head of the sensor was fitted to seal the chamber until equilibrium was reached, and the detector reading was recorded. The Aw values were obtained with ±0.001 accuracy (Zambrano et al., 2022).

2.3.3. Water-holding capacity (WHC)

The WHC was determined according to the method described by Torres et al. (2019) with modifications. Before analysis, the baked gluten-starch matrices were ground and sieved using a 12-mesh sieve. Subsequently, 2.5 g of sample was dissolved with 12 mL of distilled water with constant agitation for 60 min at 37 °C under water-excess conditions, maintaining a sample-water ratio of 1:5. After centrifugation at 3000 rpm for 10 min, the sediment was weighed (as wet weight, $W_{wet\ weight}$) and dried to constant weight (as dry weight, $W_{dry\ weight}$) in a forced-air oven at 110 °C. The WHC was determined using Eq. (1):

$$WHC\left(\frac{g}{g}\right) = \frac{W_{wet\ weight} - W_{dry\ weight}}{W_{dry\ weight}} \quad (1)$$

2.4. Gelatinization degree analysis

The gelatinization properties of laminated dough and baked gluten-starch matrices were analyzed by Differential Scanning Calorimetry (DSC) using a DSC-1 instrument (Mettler-Toledo, Greinfensee, Switzerland) along with STARe® thermal analysis software, version 13.00. The instrument was calibrated using indium as a standard (melting temperature of 156.6 ± 1.56 °C and melting enthalpy ΔH = 28.6 ± 1 $J.g^{-1}$). The assays ensured the same starch proportion in all samples (6 mg, db). Therefore, dough contents (between 11.3 and 13.3 mg) and baked matrices (between 7.4 and 8.7 mg) were weighed. The samples were placed into aluminum pans of 100 μL (Part N° ME-51119872), and distilled water was added to yield a water-to-sample ratio of 5:1 (starch in excess water). Next, DSC pans were hermetically sealed using a universal crimper press and kept at room temperature for 12 h (Contardo et al., 2020). Measurements were performed from 30 to 90 °C, with a constant heating rate of 10 °C/min. An empty aluminum pan was used as a reference. The endothermic transition temperatures (°C): onset (T_o), peak (T_p), endset (T_e), temperature range (T_e - T_o), and gelatinization enthalpy changes (ΔH, $J{\cdot}g^{-1}$) were obtained from DSC thermograms. The transition enthalpies (ΔH) associated with starch gelatinization of the dough (ΔH_{dough}) and the baked gluten-starch matrices ($\Delta H_{matrices}$) were calculated from the DSC curve (Zheng et al., 2021). The gelatinization degree (GD) of starch was calculated using eq. (2):

$$GD\ (\%) = \left(\frac{\Delta H_{dough} - \Delta H_{matrices}}{\Delta H_{dough}}\right) \quad (2)$$

where (ΔH_{dough}) corresponds to the enthalpy of all the starch granules embedded in the dough, which were forced to gelatinize in excess water, and ($\Delta H_{matrices}$) corresponds to the enthalpy of the starch granules that did not complete the gelatinization process after baking. Therefore, (ΔH_{dough} - $\Delta H_{matrices}$) denotes the enthalpy of the gelatinized starch fraction during baking (Molina et al., 2021).

2.5. Mechanical and structural tests

2.5.1. Texture profile analysis

Before baking, a texture profile analysis (TPA) of the laminated dough was conducted using a TA-XT plus texturometer (Stable Micro Systems Ltd., Godalming, Surrey, UK), following the method developed by Jiang et al. (2019) with some modifications. The device had a load cell capacity of 5 kg, a heavy-duty aluminum platform (HDP/90), and a compression platform with a 100 mm diameter (P/100). Cylinder-shaped pieces of 15 g of weight (dimensions: 10 mm in diameter and 15 mm in height) were obtained from the central part of the sample using a metal cutter. The tests were performed at 25 °C with a 5 $mm.s^{-1}$ speed and up to 40% strain level. These parameters were set according to the literature and based on preliminary experiments to prevent the destruction of the samples and accurately calculate the textural properties (Torres et al., 2019). A double compression simulating the human bite with a delay time of 10 s was performed. The parameters used as textural indicators were hardness (N), adhesiveness (N·mm), cohesiveness (dimensionless), springiness (dimensionless), and chewiness (hardness × cohesiveness × springiness, N). All variables were calculated from the TPA curve (Zhu, Tao, Wang, & Xu, 2023).

2.5.2. Three-point bending test

After baking, the textural changes were evaluated using a three-point

bending (TPB) test with modifications, following the procedure described by Dueik et al. (2014) with some changes. The analysis was conducted using a TA-XT plus with a 5 kg cell. Each sample was placed on two parallel edges (with a support span of 16 mm) to apply the load centrally. A 2.5 mm-thick steel blade with a flat edge was used to fracture the samples at a 10 mm.s^{-1} speed. The measurements were made at 25 °C, and hardness was obtained as the maximum force (N). All data were processed using texture expert software, version 1.16 for Windows (Stable Micro Systems Ltd., Surrey, UK).

2.5.3. Field emission scanning electron microscopy

The external morphology of the baked gluten-starch matrices was analyzed with a field emission scanning electron microscope (FE-SEM) (Quanta FEG250, FEI Corporate, Hillsboro, OR USA) in high-vacuum mode with a secondary electron detector. This technique provides ultra-high-resolution imaging at low accelerating voltages and small working distances (Han, Ma, Li, Zheng, & Wang, 2019). Before imaging, all baked samples were coated with a thin layer of gold (10 nm) using a high-resolution Sputter Coater (208HR, Cressington Scientific Instruments, Watford, UK) for 1 min to improve sample conductivity and aid secondary electron emission. The assays were performed at a pressure lower than 6 × 10^{-4} Pa, with an accelerating voltage of 5 kV, a working distance of 12.3 mm, and a resolution of 2 nm. The micrographs were captured in 16-bit depth (RGB), and images of 1536 × 1103 pixels were stored in TIFF format. Magnifications ranged from 2000× and 3000× to examine the external surface to 100× to 1000× to observe the cross-sections. Micrograph processing was performed using the public domain software package ImageJ® (1.52u, National Institutes of Health, MD., USA) and the free & open-source image editor GIMP® (version 2.10.24, GIMP team, Berkeley, CA, USA).

2.5.4. X-ray micro-computed tomography

The inner structure of baked gluten-starch matrices was further characterized non-destructively using X-ray micro-computed tomography (micro-CT) (Skyscan 1272, version 1.1.7, Bruker Corp., Kontich, Belgium), as illustrated in Fig. 1a, operating at 40 kV with a constant current of 250 μA. The experimental conditions were optimized for an image pixel size of 5.99 μm, encompassing 2016 × 1344 pixels per image, to achieve a low scanning time (38 min per sample).

The samples were scanned from 0 to 360° with a rotation step of 0.25° and an exposure time per frame of 500 ms. No filter was used during processing, as correction filters corrected beam-hardening defects (Contardo & Bouchon, 2018). Approximately 1300 projection images were processed to obtain reconstructed cross-section photographs (16 bit-depths) using NRecon® software (version 1.7.4.2, Bruker Corp., Kontich, Belgium), employing a modified Feldkamp algorithm (Schoeman et al., 2016). The total reconstruction time was around 465 s per sample.

During the reconstruction phase, various parameters were adjusted to ensure good quality reconstructed images, including *thermal correction* (X/Y alignment with a reference scan), *misalignment compensation* (post-alignment = 1), *smoothing* (1, using Gaussian Kernel = 2), *ring*

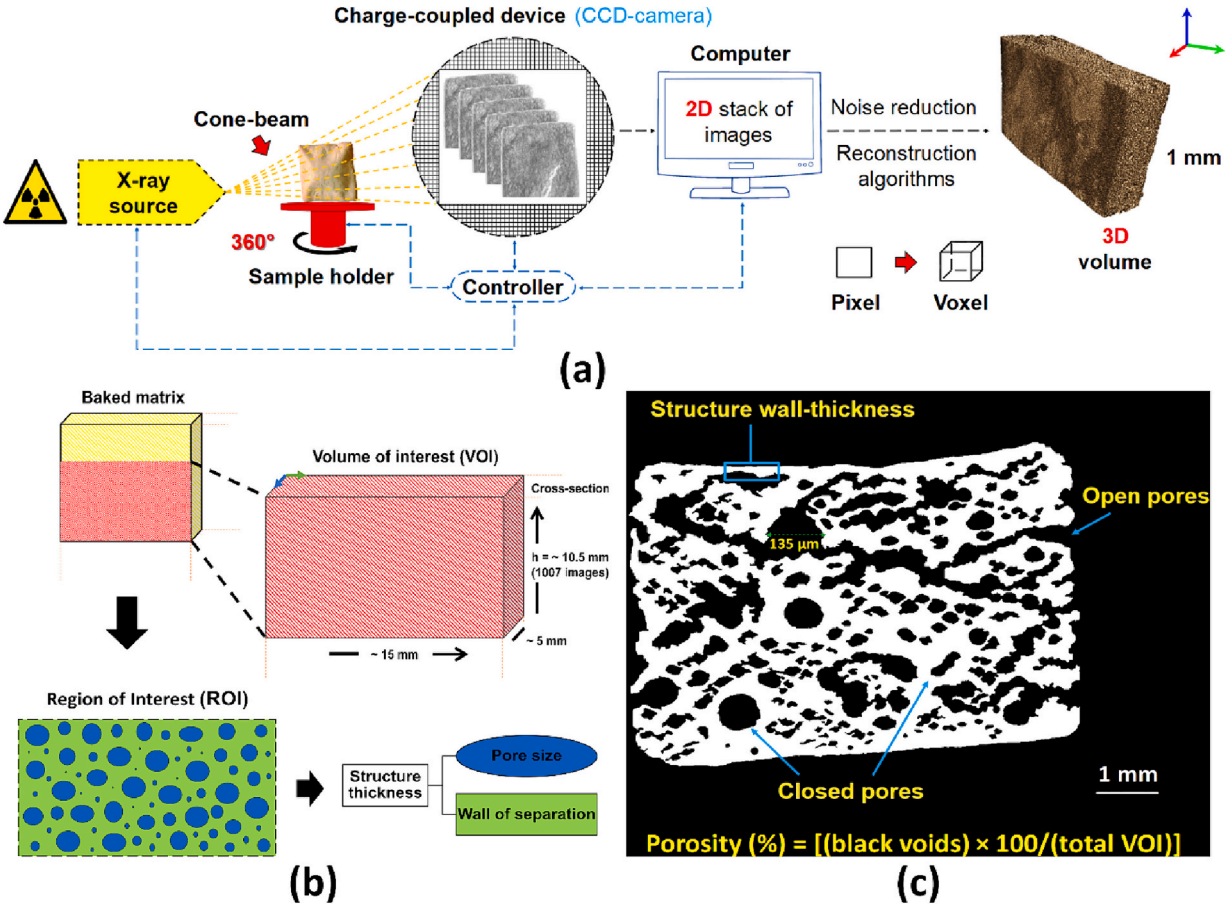

Fig. 1. Micro-CT scanning process and image analysis of baked gluten-starch matrices. (a) Diagram of the Skyscan 1272 system used. The device comprised an X-ray source, a sample holder with rotation, a controller, a cooled charge-coupled device (CCD camera), and a computer. The scanner captures 2D shadow projection images from the samples and the reconstruction process (3D volume). (b) The volume of interest (VOI) was set with 1007 cross-section images (75% of the entire samples), considering a height of 10.5 mm. A rectangular-shaped region of interest (ROI) was adjusted, and the morphometric parameters (*i.e.*, pore size or diameter and wall of separation) were calculated by applying the structure thickness method (*i.e.*, skeletonization and sphere-fitting). (c) Typical representation of the porosity: open and closed pores (Contardo et al., 2020; Contardo & Bouchon, 2018; Molina et al., 2021; Olakanmi et al., 2023; Zambrano et al., 2022).

artifact correction level (= 15), *beam hardening correction* (= 40%), *cross-section rotation* (23.16°), and *maximum for cross-section to image conversion* (= 0.11). A rectangular-shaped region of interest (ROI) was defined for all samples. A volume of interest (VOI) of 1007 slices in BMP file format (about 75% of the entire piece) was considered during the 3D quantification, as shown in Fig. 1b. The reconstructed images were processed and analyzed using CTAn® software (version 1.18.8.0, Bruker Corp., Kontich, Belgium). To do so, the volume of interest (VOI) was selected, and the noise was removed mainly using global thresholding and despeckling, median 2D, and Gaussian 3D filters. The region of interest (ROI) was defined to outline the boundary of all objects and cut lumps before segmentation.

Subsequently, morphometric parameters were determined, including (Fig. 1c) total porosity, open porosity, closed porosity, surface of pores, structure separation, and structure thickness, which corresponded to the average solid structure (distance, μm) separating the pores (wall-thickness or wall of separation) (Van Dyck et al., 2014). In contrast, structure separation indicated the average local thickness (length, μm) of the voids (also referred to as pore size or pore diameter). CTvox® volume rendering software (version 3.3.0 Bruker Corp., Kontich, Belgium) was used to show reconstructed images as realistic 3D objects.

2.6. In vitro starch digestibility

An *in vitro* digestion assay was conducted following the Englyst enzymatic method (Contardo et al., 2016). The baked gluten-starch matrices were milled and sieved.

Step 1: 1.5 g of the samples were mixed with 5 mL of a 50% saturated benzoic solution and 10 mL of pepsin-guar gum solution (5:5 g in 100 mL HCl to 0.05 M). Guar gum was added to standardize the viscosity of the fluid. The pH was maintained between 2.3 and 2.6. The tubes were mixed in a vortex, placed in a water bath, and gently shaken for 30 min at 37 °C to induce protein hydrolysis. Five mL of 0.5 M sodium acetate buffer solution (pH 5.2 ± 0.2) and five glass balls (15 mm diameter) were added to each tube. The containers were shaken and kept in the water bath for 3 min to mechanically disrupt the structure of the sample during the incubation period.

Step 2: Five mL of pancreatin-amyloglucosidase-invertase fresh enzyme mixture (18 g, 4 mL, and 60 μg, respectively, per 100 mL enzyme mixture) were added to each tube, which was capped with parafilm®, gently mixed, placed horizontally in the water bath at 37 °C, and subjected to shaking (137 rpm) to mimic peristaltic movements during digestion in the small intestine. Under these conditions, each tube was removed at 20 and 120 min. The hydrolysis was stopped by adding 0.2 mL into 4 mL of absolute ethanol, resulting in two fractions extracted at 20 min (G_{20}) and 120 min (G_{120}), respectively. The tubes were vigorously vortex-mixed for 1 min, placed in boiling water for 30 min, and then cooled in an ice-water bath for 15 min.

Step 3: Ten mL of a potassium hydroxide solution (7 M) was added to the polypropylene tubes, placed horizontally in an ice-water bath, and shaken for 30 min. Subsequently, 0.2 mL of the mixture was added to 1 mL of acetic acid (1 M), and 40 μL of amyloglucosidase from *Aspergillus niger* solution (1:7 dilution) was added. The tubes were vigorously vortex-mixed and kept at 70 °C in a water bath for 30 min, followed by 10 min in boiling water. The containers were cooled in an ice-water bath for 15 min until they reached room temperature. Next, 12 mL of absolute ethanol was added to obtain the total glucose (TG) fraction. G20, G120, and TG fractions were measured using a glucose oxidase and peroxidase GAGO-20 assay kit (Sigma-Aldrich, St Louis, MO, USA.). The absorbance was quantified at 540 nm against a reagent blank using a UV–visible spectrophotometer (model-2601, Beijing Instrument Industry Co., Ltd., Chaoyang, China). Target concentrations were calculated by plotting a standard curve through known glucose solution concentrations (Zhou et al., 2021). *Rapidly available glucose* (RAG), *slowly available glucose* (SAG), and *unavailable glucose* (UG) fractions (g/100 g) were estimated in the following eqs. (3, 4, and 5):

$$\mathrm{RAG}\left(\frac{g}{100g}\right) = \left(\frac{G_{20}}{TG}\right) x\ 100 \tag{3}$$

$$\mathrm{SAG}\left(\frac{g}{100g}\right) = \left(\frac{G_{120} - G_{20}}{TG}\right) x\ 100 \tag{4}$$

$$\mathrm{UG}\left(\frac{g}{100g}\right) = \left(\frac{TG - G_{120}}{TG}\right) x\ 100 \tag{5}$$

2.7. Statistical analysis

Physicochemical, microstructural assays and starch digestibility results correspond to the arithmetic mean of three batches per formulation ± standard deviation unless otherwise specified. Texture measurements were performed six times for each set. A one-way analysis of variance (ANOVA) with the *post-hoc* HSD Tukey test at 5% significance was used to analyze mean value differences. The data were processed using the Statgraphics Centurion program (version 16.2.04, Stat-Point Technologies Inc., USA).

3. Results and discussion

3.1. Effect of inulin and polydextrose on textural properties of dough

It has been claimed that IN and PD influence the textural properties and sheetability in dough systems (Ahmed, Thomas, & Khashawi, 2020; Samakradhamrongthai, Maneechot, Wangpankhajorn, Jannu, & Renaldi, 2022); therefore, understanding this impact is relevant. Table 2 presents the textural parameters and moisture changes in the starchy matrices with and without IN and PD before and after baking. The TPA indicated a significant increase in the hardness of laminated dough when the concentration of IN and PD was raised ($p < 0.05$). Hardness ranged from 13.33 N in the control dough (model matrix made of gluten and starch) to 38.97 N and 66.75 N in samples with 13% IN or 13% PD, respectively. A similar trend was observed in chewiness, which showed a four-fold increase compared to the control dough when PD was added. These results suggest that the addition of IN or PD strengthens the dough structure, which is consistent with the findings of Kiumarsi et al. (2019), who reported that adding 7.5% IN reinforces the structure of bread dough. As observed by the authors, this phenomenon could be attributed to the higher development of the protein network promoted by adding SDFs (Zhou et al., 2021). Notably, a more stable gluten network could enhance dough stability during storage and processing (Zhou et al., 2022).

Cohesiveness refers to the intermolecular attractions by which a food matrix is held together (Ahmed et al., 2020). Adding SDFs did not affect dough formation during mixing, allowing consistent and flexible structures. No statistical differences in the cohesiveness of laminated dough with and without IN and PD were obtained ($p > 0.05$). These findings suggest that neither the type of SDF nor the concentration used in the formulation affects the internal cohesion of the laminated dough. Preserving dough cohesiveness is relevant, given that it serves as an exceptional predictive parameter of bread quality (Jiang et al., 2019).

SDF addition affected the adhesiveness of laminated dough, substantially reducing it when adding IN or PD; however, no differences were found when comparing concentrations of 7.5 and 13% ($p > 0.05$) for each SDF. Adhesiveness notably increased in samples with PD ($p < 0.05$), indicating a stickier behavior that was more challenging to handle during kneading. This behavior could be linked to more significant water absorption by SDF and the formation of a gel-like structure, resulting in an increase in viscosity (Chen et al., 2020; Zhou et al., 2021). This pattern aligns with water activity (Aw) measurements, which indicated a significant reduction when adding SDF ($p < 0.05$). No statistical differences ($p > 0.05$) in Aw were found when adding either IN or

Table 2
Texture profile analysis and water activity of laminated doughs, prepared with gluten (12%) and starch (88%) as the control dough or by replacing starch with 7.5 or 13 g/100 g inulin (IN7.5% or IN13%) or polydextrose (PD7.5% or PD13%), including the evaluation of texture, water retention, and starch gelatinization degree after baking.

Matrix	Method	Parameters	Starchy formulations				
			Control	IN7.5%	IN13%	PD7.5%	PD13%
Laminated dough	Texture profile analysis (TPA)	Hardness (N)	13.33 ± 2.83a	32.19 ± 6.03b	38.97 ± 5.41b	63.47 ± 9.76c	66.75 ± 6.43c
		Chewiness (N)	9.57 ± 2.53a	20.88 ± 4.78b	24.32 ± 3.71b	40.39 ± 4.16c	38.27 ± 5.48c
		Cohesiveness (Dimensionless)	0.73 ± 0.16a	0.69 ± 0.13a	0.65 ± 0.18a	0.67 ± 0.12a	0.63 ± 0.14a
		Adhesiveness (N·mm)	−0.53 ± 0.09a	−1.97 ± 0.56b	−2.62 ± 0.22b	−4.34 ± 0.34c	−4.02 ± 0.51c
		Springiness (Dimensionless)	0.97 ± 0.03a	0.94 ± 0.04a	0.96 ± 0.03a	0.95 ± 0.04a	0.91 ± 0.06a
	Electric hygrometer	Aw (25 °C)	0.963 ± 0.042b	0.843 ± 0.045a	0.811 ± 0.084a	0.851 ± 0.031a	0.819 ± 0.057a
Baked matrices	Three-point bending	Maximum breaking force (hardness, N)	27.84 ± 6.55a	53.91 ± 3.57c	62.82 ± 6.47d	39.73 ± 4.43b	43.85 ± 5.82b
	Centrifugation	WHC (g/g)	0.93 ± 0.06a	1.76 ± 0.28b	2.58 ± 0.31c	1.64 ± 0.32b	1.97 ± 0.44bc
	Differential scanning calorimeter (DSC)	Starch gelatinization degree (%)	69.28 ± 3.34c	63.84 ± 2.25b	51.24 ± 4.11a	62.84 ± 2.82b	54.92 3.79a

Data are means ± standard deviation (n = 3, and $n = 6$ for texture parameters). Different superscripts ($p < 0.05$) in the same row denote significant differences ($p < 0.05$).

PD, regardless of the concentration used. Comparable outcomes were reported by Rodríguez-García, Laguna, Puig, Salvador, and Hernando (2013), who observed a decrease in Aw in dough biscuits with IN, and by Samakradhamrongthai et al. (2022), who noted a slight decrease in Aw with PD addition in cookie formulations.

No statistical differences in springiness were found ($p > 0.05$), indicating that dough formulations returned to their original shape after the deforming force was removed (Han et al., 2019). Springiness refers to the height recovered by the sample after deformation (Jiang et al., 2019), where values near the unit signify proper flexibility and resistance, while values near zero are associated with a weak structure that deforms rapidly (Zhu et al., 2023).

3.2. Effect of inulin and polydextrose on texture, water retention, and the starch gelatinization degree after baking

After baking, a significant effect of the type of SDF and the concentration used on the hardness (maximum breaking force) of starchy matrices was found ($p < 0.05$). The hardness of baked matrices increased with the addition of IN and PD, and this effect was more pronounced at higher SDF concentrations, reaching maximum values when adding 7.5 or 13% IN (53.91 and 62.82 N, respectively). These findings are consistent with Samakradhamrongthai et al. (2022), who said that PD addition significantly increased the hardness of cookies with a range between 58.96 and 129.20 N. According to Zhou et al. (2021), this behavior could be attributed to the strong interaction of SDF with the gluten network, leading to increased compactness in the food matrix.

Regarding water-holding capacity (WHC), the experimental results indicated that the addition of IN or PD caused an increase in all formulations ($p < 0.05$). Overall, matrices with IN showed higher WHC than formulations with PD at both concentrations, with an increase of up to 2.58 (g/g) in samples with 13% IN. These findings suggest that IN and PD could capture water in the dough structure, limiting its availability and thereby influencing the starch gelatinization degree and the texture of baked matrices (Zhu et al., 2023). Furthermore, the WHC of baked samples could help understand their hydration behavior during *in vitro* starch digestibility.

The gelatinization degree (GD) of the different baked gluten-starch matrices was further determined to understand the effect of SDF addition in the formed doughs. As shown in Table 2 (last row), GD was significantly lower in formulations containing SDF compared to the control ($p < 0.05$). Moreover, the reduction increased with the concentration of SDF. The highest reduction was found in formulations with 13% IN, exhibiting a ~ 26% decrease, followed by samples with 13% PD, which had an average drop of ~21% and was not significantly different from the former. Starchy matrices with 7.5% PD and 7.5% IN decreased GD by ~9.3 and ~ 7.9%, respectively, compared to the control dough, and no significant differences were found between them ($p > 0.05$). Starch gelatinization requires sufficient liquid water and temperature (heating); thus, a reduction in GD in the presence of IN and PD at different concentrations may be related to decreased water availability in the dough systems. The lower water activity of the matrices formulated with IN or PD can be linked to a decreased GD. A positive correlation was obtained between Aw and GD ($r = 0.85$). Several authors have stated that a high GD is associated with increased starch susceptibility to hydrolysis by digestive enzymes due to higher exposure to starch molecules (Chen et al., 2020). In contrast, a lower GD could hinder amylolysis (Zhou et al., 2022), as will be discussed further.

3.3. Effect of inulin and polydextrose addition on structural changes of baked gluten-starch matrices

Microstructural changes play a crucial role in the physical characteristics of starchy foods (Aguilera, 2022). Since most recognizable elements are below the 100 μm range, microscopy is vital, especially non-invasive techniques such as X-ray micro-computed tomography (micro-CT). Fig. 2 shows the 2D representation of the cross-section (left-hand side) and the 3D reconstruction (right-hand side) of baked gluten-starch matrices obtained through micro-CT scanning. The image analysis revealed that the control matrices had the highest ($p < 0.05$) porosity (69.12%). This value decreased significantly by ~23 and 25% in samples with 7.5% PD or IN, respectively, and by around ~33 and 37% in models with 13% PD or IN; no significant differences were found when comparing the different SDFs at each concentration. The control matrices exhibited remarkable cracks (voids) with much larger pores than those in matrices containing SDFs, where most pores ranged between 366 and 616 μm. Image analysis indicated a more compact structure with fewer fissures when IN or PD were added, particularly at their highest concentration.

In formulations with 7.5% IN or PD, the highest number of pores shifted towards smaller ranges, compared to the control matrix, with maximum values (~40%) in the 126–246 μm range. This pattern was enhanced as the concentration of IN or PD increased up to 13%, where the smaller size range (6–126 μm) accounted for nearly 40% of total

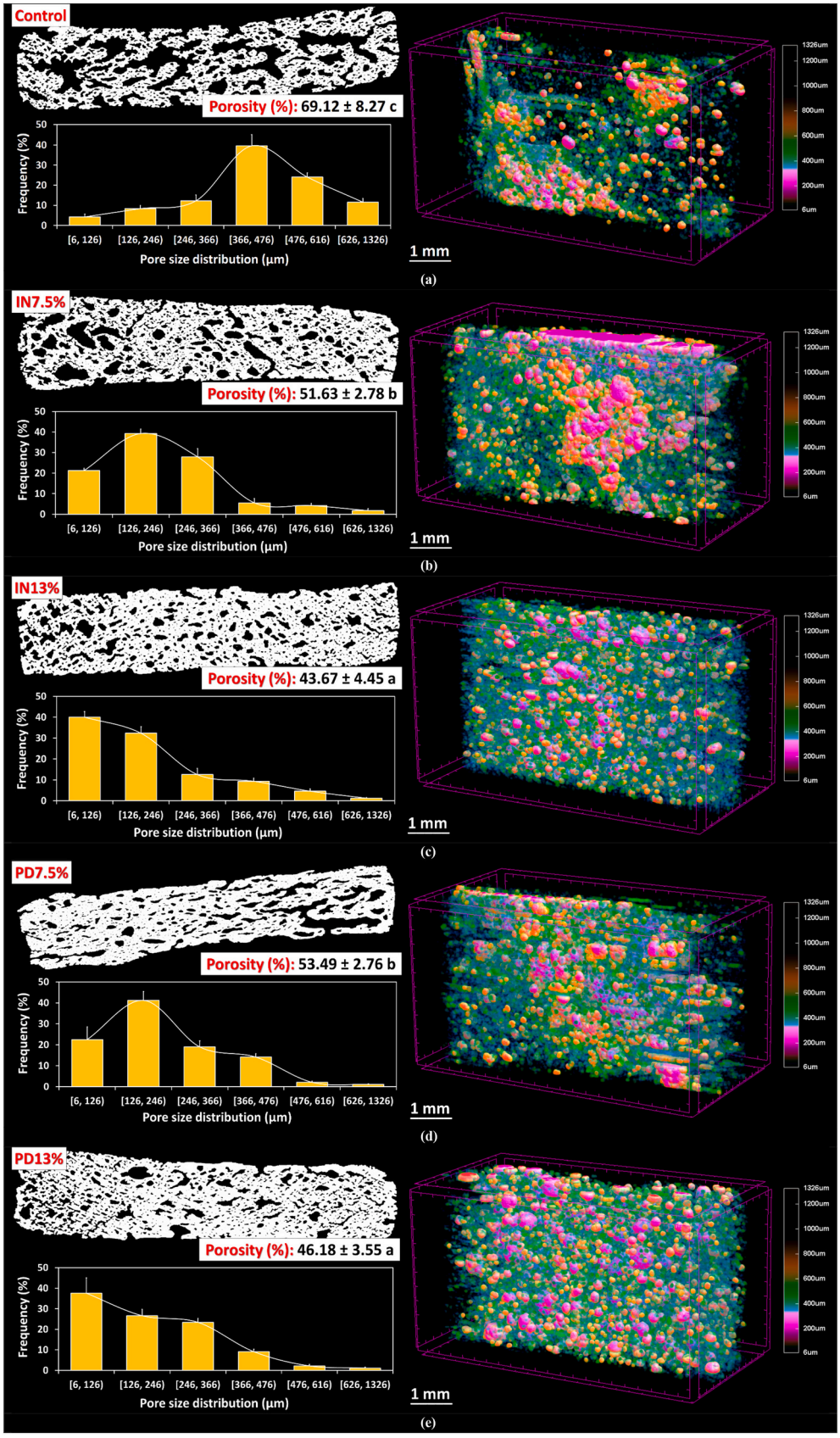

Fig. 2. Total porosity, pore size distribution, 2D cross-section representations, and 3D reconstructed images of baked gluten-starch matrices prepared with gluten (12%) and starch (88%) as the control dough or by replacing starch with 7.5 or 13 g/100 g inulin (IN7.5% or IN13%) or polydextrose (PD7.5% or PD13%), obtained through micro-CT scanning, with different letters indicating significant difference ($p < 0.05$).

pores. These findings concur with Van Dyck et al. (2014), who found more tiny pores in bread with wheat bran despite the differences between the two systems. The lower porosity development during the baking of starchy models with IN or PD could be associated with a less vigorous escape of water from the inner structure due to higher water retention by these SDFs (Wang et al., 2023).

To gain a deeper understanding of the impact of IN or PD addition on matrix microstructure, some key morphometric parameters obtained from micro-CT image analysis are shown in Table 3. Regarding the structure thickness (St.Th), a significant increase was observed with the addition of both IN and PD ($p < 0.05$). It varied from 40.73 μm in the control samples to 112.37 μm in model matrices with 13% PD and up to 128.14 μm in pieces with 13% IN, according to porosity results. These samples exhibited a denser structure, lower porosity, and a more significant structure thickness than the control. Additionally, the mean pore diameter (Po·D) significantly decreased in the presence of IN or PD. At higher concentrations, it decreased from 393.26 μm in control samples to 80.35 μm and 74.98 μm in pieces with 13% PD or IN, respectively ($p < 0.05$), as inferred from the pore size distribution (Fig. 2 left-hand side).

Porosity is linked to textural properties and influences the mechanical behavior of starchy foods (Chen et al., 2021). As previously mentioned, open pores (Po.op) indicate voids connected to other holes and the external environment, while closed pores (Po.cl) are surrounded by solid structures (Olakanmi et al., 2023). The control matrix exhibited a higher proportion of Po.op, accounting for 67.15% ($p < 0.05$), and a lower Po.cl, accounting for 1.97% ($p < 0.05$). Adding IN or PD at the highest levels caused a significant decrease in Po.op, reaching 38.62% and 40.02% in the formulations with 13% IN or PD, respectively. Moreover, these formulations showed the highest values of Po.cl, representing approximately 5.05% and 6.16%, respectively ($p < 0.05$).

These results concur with Van Dyck et al. (2014), who indicated Po.cl and Po.op values of 0.40% and 82.63% in white bread, respectively. Similarly, Jeong, Park, and Lee (2021) found a higher proportion of Po.op (66.55%) than Po.cl (0.02%) in the wheat dough. Overall, it has been reported that the ratio of Po.cl is always lower than Po.op in starchy foods. Besides providing information about the internal structure, a proper understanding of porosity (Po.op and Po.cl) in baked gluten-starch matrices could help in designing other bakery food matrices with improved textural attributes (Chen et al., 2021). Altogether, these results may be linked to the differences in the hardness of baked matrices reported in Table 2. As porosity decreased, the St.Th increased when SDFs were added, and the external structure of the baked matrices became more rigid and difficult to break.

In addition, FE-SEM observations were performed to examine morphological changes of starch granules upon baking. Fig. 3 shows representative micrographs of the surface (left-hand column) and cross-sections (right-hand column) of the different baked gluten-starch matrices with and without IN or PD addition. Similar patterns concerning porosity (P in Fig. 3) were observed compared to those obtained through micro-CT when analyzing the different cross-sections. Higher voids are seen in the control matrix, resulting in a higher concentration of smaller ones as SDFs are added. The external surface shows that all samples contained a gluten matrix (G in Fig. 3) embedding the gelatinized starch granules (S in Fig. 3).

It is also evident that starch granules suffered different morphological changes related to the different swelling patterns and partial gelatinization. Some granules retain their structural characteristics significantly, while others became irregular, losing their oval shape. Starch granules exhibited higher deformations in control samples, displaying a depression in the center or a more prominent elongation than model matrices with SDFs. In samples with IN or PD addition, starch granules appeared wrapped by a close-fitting adherent layer on the surface (FC in Fig. 3). IN or PD may create a coating over the starch granules, which can hinder starch gelatinization, allowing them to preserve their original shape to a greater extent. In this regard, Wang et al. (2021) indicated that the addition of bamboo shoots dietary fiber formed a "*barrier*" on the starch surface, protecting them from gelatinization. Similar behaviors have been suggested by Han et al. (2019) when analyzing the impact of wheat dietary fiber on starch gelatinization in gluten-starch systems. They reported that the fiber may wrap starch granules, preventing gelatinization. Indeed, these observations and behaviors may affect starch digestibility, as will be analyzed in the next section.

3.4. *Effect of inulin and polydextrose on in vitro starch digestibility of baked gluten-starch matrices*

The physical state of starch, food microstructure, and specific interactions with certain biomolecules may affect starch digestibility (Tian et al., 2019; Toutounji et al., 2019). Fig. 4 shows the impact of IN or PD addition on *in vitro* starch digestibility, expressed in terms of the fractions of glucose released from the baked gluten-starch matrices over time, distinguishing the *rapidly available* (RAG in Fig. 4a), the *slowly available* (SAG in Fig. 4b), and the *unavailable* (UG in Fig. 4c) glucose fractions.

The control matrices presented the highest RAG values, accounting for 34.85 g/100 g. This value decreased significantly ($p < 0.05$) up to 18.92 g/100 g and 8.56 g/100 g in samples with 7.5% and 13% IN, respectively, and dropped to 15.21 g/100 g and 15.13 g/100 g in model samples with 7.5% and 13% PD, respectively. The SAG fraction was significantly lower than the RAG fraction in all formulations ($p < 0.05$) and decreased compared to the control sample as IN or PD was added. Furthermore, the amount of UG increased significantly as SDF was added ($p < 0.05$), rising from 47.59 g/100 g in control samples up to twice this amount (87.76 g/100 g) in matrices with 13% IN. No significant differences ($p > 0.05$) in the different glucose fractions were obtained in samples with 7.5% or 13% PD. Conversely, the RAG and SAG fractions were significantly lower, and the UG fraction was significantly higher ($p < 0.05$) in samples with 13% IN compared to those prepared with 7.5% IN.

The decrease in RAG and the consequent increase in UG in samples with IN or PD addition may be explained, to some extent, by the lower gelatinization degree of starch found in these samples (Table 2), as ungelatinized starch is barely digestible, as previously discussed. This behavior could also be enhanced by the "*physical barrier*" that the SDF

Table 3
3D morphometric parameters of baked gluten-starch matrices prepared with gluten (12%) and starch (88%) as the control dough or by replacing starch with 7.5 or 13 g/100 g inulin (IN7.5% or IN13%) or polydextrose (PD7.5% or PD13%) from micro-CT image analysis.

Morphometric parameters	Abbreviation	Baked gluten-starch matrices					Unit
		Control	IN7.5%	IN13%	PD7.5%	PD13%	
Total VOI volume	TV	787.50 ± 30.72 a	751.93 ± 45.11 a	757.91 ± 37.93 a	752.87 ± 41.47 a	756.43 ± 36.36 a	mm^3
Structure wall-thickness	St.Th	40.73 ± 6.29 a	70.27 ± 3.09 b	128.14 ± 16.02 c	61.83 ± 6.69 b	112.37 ± 20.21 c	μm
Pore diameter	Po·D	393.26 ± 90.61 c	118.69 ± 23.56 b	74.98 ± 12.09 a	161.37 ± 40.42 b	80.35 ± 7.88 a	μm
Open porosity	Po.op	67.15 ± 8.03 c	48.81 ± 2.39 b	38.62 ± 5.18 a	51.21 ± 3.64 b	40.02 ± 2.65 a	% (V/TV)
Closed porosity	Po.cl	1.97 ± 0.29 a	2.82 ± 0.83 b	5.05 ± 1.32 c	2.28 ± 0.26 b	6.16 ± 1.21 c	% (V/TV)

Data are the mean values ± standard deviation (n = 3). Different letters in the same row denote significant differences ($p < 0.05$).

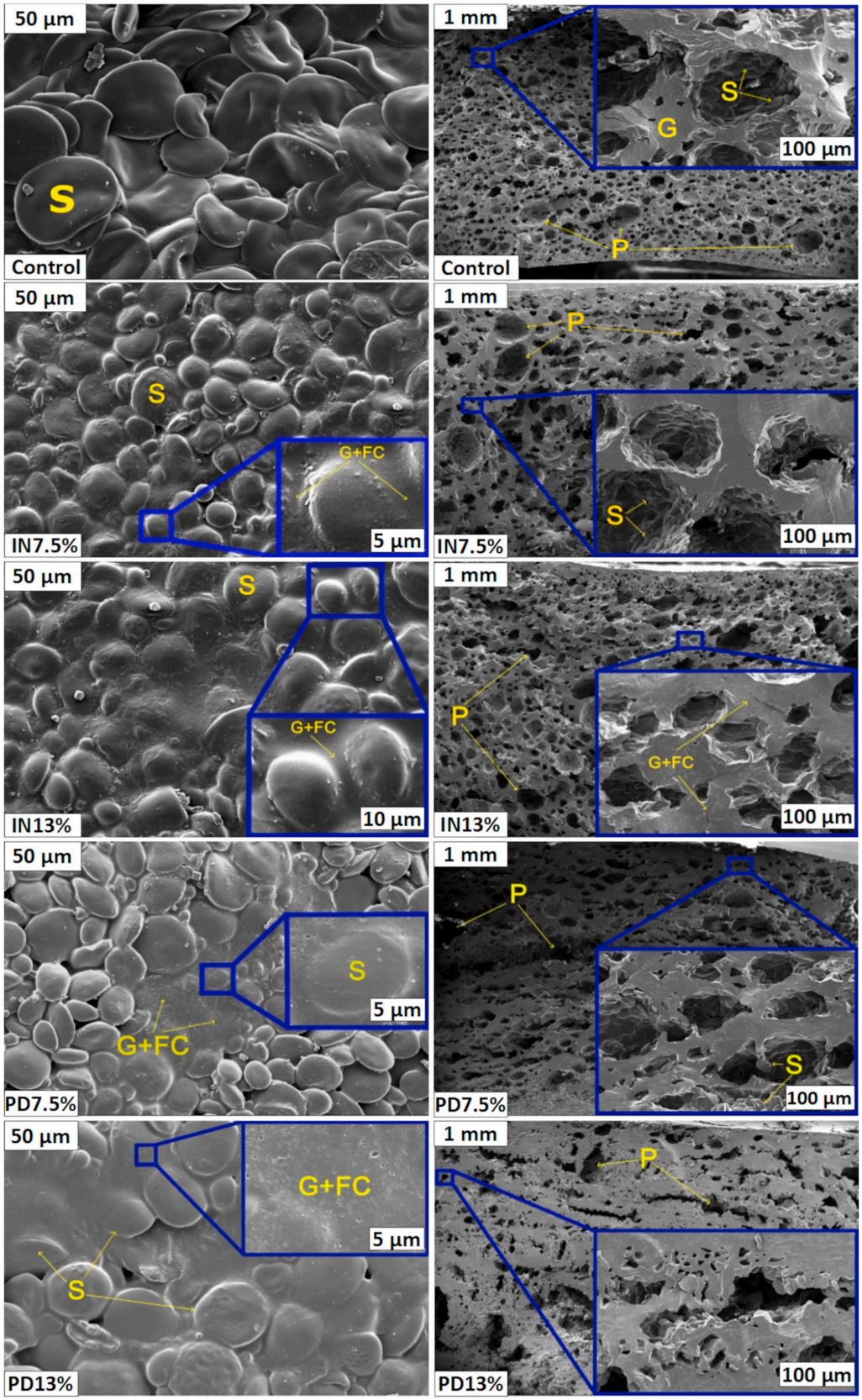

Fig. 3. FE-SEM images of baked gluten-starch matrices prepared with gluten (12%) and starch (88%) as the control dough or by replacing starch with 7.5 or 13 g/100 g inulin (IN7.5% or IN13%) or polydextrose (PD7.5% or PD13%). The letters refer to G: gluten; S: Starch; P: pores; FC: fiber coating. Images on the left column correspond to the external surface, while images on the right column correspond to the sample cross-section.

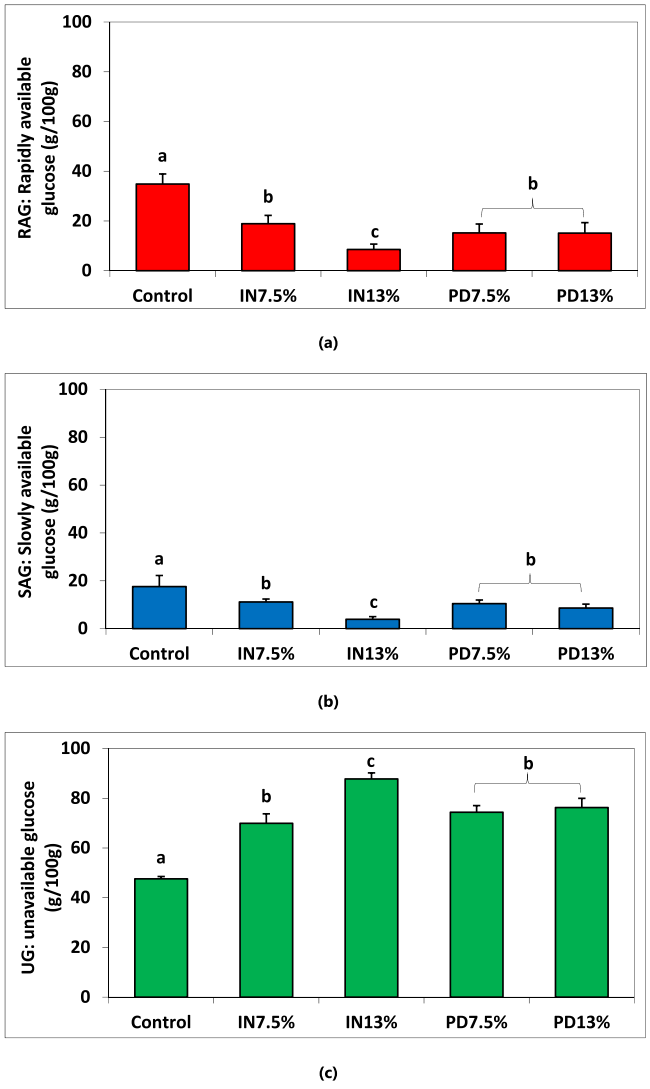

Fig. 4. *Rapidly available* (RAG), *slowly available* (SAG), and *unavailable glucose* (UG) fractions after *in vitro* digestion of baked gluten-starch matrices prepared with gluten (12%) and starch (88%) as the control dough or by replacing starch with 7.5 or 13 g/100 g inulin (IN7.5% or IN13%) or polydextrose (PD7.5% or PD13%). Data are the mean values ± standard deviation ($n = 3$). Different superscripts denote significant differences ($p < 0.05$).

coating over starch granules can confer, which may not only preclude gelatinization but also limit starch digestibility, as revealed by FE-SEM (Fig. 3). In addition, the lower porosity and higher packed structure found in samples with SDFs (Fig. 2) could also contribute to a decrease in starch digestibility.

Overall, no significant differences in fractions were observed when comparing samples with PD at any concentration and those with 7.5% IN concentration. However, a significantly lower RAG fraction and a considerably higher UG fraction were obtained in samples with 13% IN. This could be attributed to microstructural effects, as IN at higher concentrations could cause a more marked physical embedding of starch granules, hindering amylolysis (Yang et al., 2023; Zhang et al., 2022). It should be emphasized that the gluten network may also act as a physical barrier, retarding or hindering the access of digestive enzymes to starch molecules (Han et al., 2019), or it may interact with starch, altering starch digestibility (Zhou et al., 2021). In this research, all baked samples had the same gluten content to avoid differences in starch digestibility between the matrices due to this factor.

It is important to note that the Englyst enzymatic method is a static method that provides information about the total amount of digested starch at specific moments and does not consider the rate of starch digestion over time, which can provide further insights (Bello-Pérez et al., 2020; Toutounji et al., 2019). This method should be considered as a first approximation and should be complemented in the future with a dynamic model to further understand how starch digestibility occurs in these systems.

4. Conclusions

The results indicate that gluten-starch formulations can be enriched with soluble dietary fiber (inulin, IN; polydextrose, PD) without compromising their sheetability, enabling proper structure formation during baking. The addition of IN or PD led to increased water-holding capacity and hardness of the baked matrices. These findings, along with the lower water activity in the formulated matrices, may be linked to the lower degree of starch gelatinization observed with increasing IN or PD concentration.

Morphological analysis of baked gluten-starch matrices with IN or PD showed a dense and compact network surrounding some gelatinized starch granules. The observed cover, combined with a decrease in total porosity, open porosity, increased structure thickness, and a lower starch gelatinization degree in the matrices, could account for the lower *in vitro* starch digestibility, which decreased as the concentration of IN or PD increased.

Enzymatic assays demonstrated a more significant reduction in the *rapidly available glucose* fraction and a significant increase in the *unavailable glucose* fraction in all baked gluten-starch matrices supplemented with IN or PD. These results suggest that gluten-starch matrices enriched with IN or PD may have a lower glycemic impact and could contribute to the development of healthier, starch-rich baked foods.

CRediT authorship contribution statement

José D. Torres: Conceptualization, Formal analysis, Investigation, Methodology, Software, Writing – original draft, Writing – review & editing. **Verónica Dueik:** Writing – review & editing, Supervision, Resources, Formal analysis. **Ingrid Contardo:** Writing – review & editing, Methodology. **David Carré:** Resources, Formal analysis. **Pedro Bouchon:** Writing – review & editing, Validation, Supervision, Resources, Project administration, Formal analysis, Conceptualization.

Declaration of competing interest

The authors declare that they have no known competing financial interests or personal relationships that could have appeared to influence the work reported in this paper.

Data availability

Data will be made available on request.

Acknowledgments

The authors thank the financial support received through FONDECYT project No. 1210709. Furthermore, the authors thank Mrs. Carla Vallejo from the X-ray micro-computed tomography laboratory (MICROCT-UC) for her technical assistance under the FONDEQUIP project EQM130028. Mr. José Galaz from the Center of Nanotechnology Research and Advanced Materials (CIEN-UC) for his technical assistance in the field-emission scanning electron microscopy (FE-SEM) assays. Finally, José D. Torres would like to thank the governorship of Bolívar-Colombia and the CEIBA Foundation for the Ph.D. scholarship granted in the call BOLÍVAR GANA CON CIENCIA.

References

Aguilera, J. M. (2022). Rational food design and food microstructure. *Trends in Food Science & Technology., 122*, 256–264. https://doi.org/10.1016/j.tifs.2022.02.006

Ahmed, J., Thomas, L., & Khashawi, R. A. (2020). Effect of inulin on rheological, textural, and structural properties of brown wheat flour dough and *in vitro* digestibility of developed Arabic bread. *Journal of Food Science, 85*(11), 3711–3721. https://doi.org/10.1111/1750-3841.15491

AOAC. Association of Official Analytical Chemists. (1995). *Official Methods of Analysis, 16th ed., sec. 975.55, Washington, DC, USA*.

Bello-Pérez, L. A., & Flores-Silva, P. C. (2023). Interaction between starch and dietary compounds: New findings and perspectives to produce functional foods. *Food Research International, 172*, Article 113182. https://doi.org/10.1016/j.foodres.2023.113182

Bello-Pérez, L. A., Flores-Silva, P. C., Agama-Acevedo, E., & Tovar, J. (2020). Starch digestibility: Past, present, and future. *Journal of the Science of Food and Agriculture, 100*(14), 5009–5016. https://doi.org/10.1002/jsfa.8955

Chen, M., Guo, L., Nsor-Atindana, J., Goff, H. D., Zhang, W., Mao, J., & Zhong, F. (2020). The effect of viscous soluble dietary fiber on nutrient digestion and metabolic responses I: In vitro digestion process. *Food Hydrocolloids, 10*(7), Article 105971. https://doi.org/10.1016/j.foodhyd.2020.105971

Chen, Y., Parrilli, A., Jaedig, F., Fuhrmann, A., Staedeli, C., Fischer, P., & Windhab, E. J. (2021). Micro-computed tomography study on bread dehydration and structural changes during ambient storage. *Journal of Food Engineering, 296*, Article 110462. https://doi.org/10.1016/j.jfoodeng.2020.110462

Chen, Z., Liang, N., Zhang, H., Li, H., Guo, J., Zhang, Y., Chen, Y., Wang, Y., & Shi, N. (2024). Resistant starch and the gut microbiome: Exploring beneficial interactions and dietary impacts. *Food Chemistry: X, 21*, Article 101118. https://doi.org/10.1016/j.fochx.2024.101118

Contardo, I., & Bouchon, P. (2018). Enhancing Micro-CT methods to quantify oil content and porosity in starch-gluten matrices. *Journal of Food Engineering, 237*, 154–161. https://doi.org/10.1016/j.jfoodeng.2018.05.038

Contardo, I., James, B., & Bouchon, P. (2020). Microstructural characterization of vacuum-fried matrices and their influence on starch digestion. *Food Structure, 25*, Article 100146. https://doi.org/10.1016/j.foostr.2020.100146

Contardo, I., Parada, J., Leiva, A., & Bouchon, P. (2016). The effect of vacuum frying on starch gelatinization and its in vitro digestibility in starch–gluten matrices. *Food Chemistry, 197*, 353–358. https://doi.org/10.1016/j.foodchem.2015.10.028

Dueik, V., Sobukola, O., & Bouchon, P. (2014). Development of low-fat gluten and fried starch matrices with high fiber content. *LWT-Food Science and Technology, 59*(1), 6–11. https://doi.org/10.1016/j.lwt.2014.04.036

Goff, H. D., Repin, N., Fabek, H., El Khoury, D., & Gidley, M. J. (2018). Dietary fiber for glycaemic control: Towards a mechanistic understanding. *Bioactive Carbohydrates and Dietary Fibre, 14*, 39–53. https://doi.org/10.1016/j.bcdf.2017.07.005

Han, W., Ma, S., Li, L., Zheng, X., & Wang, X. (2019). Impact of wheat bran dietary fiber on gluten and gluten-starch microstructure formation in dough. *Food Hydrocolloids, 95*, 292–297. https://doi.org/10.1016/j.foodhyd.2018.10.033

Jeong, S., Park, Y., & Lee, S. (2021). Assessment of turanose as a sugar alternative in a frozen dough system: Rheology, tomography, and baking performance. *LWT - Food Science and Technology, 141*, Article 110869. https://doi.org/10.1016/j.lwt.2021.110869

Jiang, Y., Zhao, Y., Zhu, Y., Qin, S., Deng, Y., & Zhao, Y. (2019). Effect of dietary fiber-rich fractions on texture, thermal, water distribution, and gluten properties of frozen dough during storage. *Food Chemistry, 297*, Article 124902. https://doi.org/10.1016/j.foodchem.2019.05.176

Kiumarsi, M., Shahbazi, M., Yeganehzad, S., Majchrzak, D., Lieleg, O., & Winkeljann, B. (2019). Relation between structural, mechanical, and sensory properties of gluten-free bread as affected by modified dietary fibers. *Food Chemistry, 277*, 664–673. https://doi.org/10.1016/j.foodchem.2018.11.015

Lim, S., Bae, J. H., Kwon, H. S., & Nauck, M. A. (2021). COVID-19 and diabetes mellitus: From pathophysiology to clinical management. *Nature Reviews Endocrinology, 17*(1), 11–30. https://doi.org/10.1038/s41574-020-00435-4

Molina, M. T., Vaz, S. M., Leiva, Á., & Bouchon, P. (2021). Rotary-moulded biscuits: Dough expansion, microstructure and sweetness perception as affected by sucrose: Flour ratio and sucrose particle size. *Food Structure, 100199*. https://doi.org/10.1016/j.foostr.2021.100199

Olakanmi, S., Karunakaran, C., & Jayas, D. (2023). Applications of X-ray micro-computed tomography and small-angle X-ray scattering techniques in food systems: A concise review. *Journal of Food Engineering, 342*, Article 111355. https://doi.org/10.1016/j.jfoodeng.2022.111355

Rodríguez-García, J., Laguna, L., Puig, A., Salvador, A., & Hernando, I. (2013). Effect of fat replacement by inulin on textural and structural properties of short dough biscuits. *Food and Bioprocess Technology, 6*(10), 2739–2750. https://doi.org/10.1007/s11947-012-0919-1

Samakradhamrongthai, R. S., Maneechot, S., Wangpankhajorn, P., Jannu, T., & Renaldi, G. (2022). Polydextrose and guar gum as a fat substitute in rice cookies and its physical, textural, and sensory properties. *Food Chemistry Advances, 1*, Article 100058. https://doi.org/10.1016/j.focha.2022.100058

Schoeman, L., Williams, P., du Plessis, A., & Manley, M. (2016). X-ray micro-computed tomography (μCT) for non-destructive characterisation of food microstructure. *Trends in Food Science & Technology*. https://doi.org/10.1016/j.tifs.2015.10.016. pp. 47, 10–24.

Sharma, P., Behl, T., Sharma, N., Singh, S., Grewal, A. S., Albarrati, A., & Bungau, S. (2022). COVID-19 and diabetes: Association intensify risk factors for morbidity and mortality. *Biomedicine & Pharmacotherapy, 113089*. https://doi.org/10.1016/j.biopha.2022.113089

Sun, H., Saeedi, P., Karuranga, S., Pinkepank, M., Ogurtsova, K., Duncan, B. B., & Magliano, D. J. (2022). IDF diabetes atlas: Global, regional, and country-level diabetes prevalence estimates for 2021 and projections for 2045. *Diabetes Research and Clinical Practice, 183*, Article 109119. https://doi.org/10.1016/j.diabres.2021.109119

Tian, J., Ogawa, Y., Shi, J., Chen, S., Zhang, H., Liu, D., & Ye, X. (2019). The microstructure of starchy food modulates its digestibility. *Critical Reviews in Food Science and Nutrition, 59*(19), 3117–3128. https://doi.org/10.1080/10408398.2018.1484341

Torres, J. D., Dueik, V., Carré, D., & Bouchon, P. (2019). Effect of the addition of soluble dietary fiber and green tea polyphenols on acrylamide formation and *in vitro* starch digestibility in baked starchy matrices. *Molecules, 24*(20), 3674. https://doi.org/10.3390/molecules24203674

Toutounji, M. R., Farahnaky, A., Santhakumar, A. B., Oli, P., Butardo, V. M., Jr., & Blanchard, C. L. (2019). Intrinsic and extrinsic factors affecting rice starch digestibility. *Trends in Food Science & Technology, 88*, 10–22. https://doi.org/10.1016/j.tifs.2019.02.012

Van Dyck, T., Verboven, P., Herremans, E., Defraeye, T., Van Campenhout, L., Wevers, M., & Nicolaï, B. (2014). Characterisation of structural patterns in bread as evaluated by X-ray computer tomography. *Journal of Food Engineering, 123*, 67–77. https://doi.org/10.1016/j.jfoodeng.2013.09.017

Wang, L., Li, Y., Guo, Z., Wang, H., Wang, A., Li, Z., & Qiu, J. (2023). Effect of buckwheat hull particle-size on bread staling quality. *Food Chemistry, 405*, Article 134851. https://doi.org/10.1016/j.foodchem.2022.134851

Wang, N., Wu, L., Huang, S., Zhang, Y., Zhang, F., & Zheng, J. (2021). Combination treatment of bamboo shoot dietary fiber and dynamic high-pressure microfluidization on rice starch: Influence on physicochemical, structural, and in vitro digestion properties. *Food Chemistry, 350*, Article 128724. https://doi.org/10.1016/j.foodchem.2020.128724

Yang, Z., Zhang, Y., Wu, Y., & Ouyang, J. (2023). Factors influencing the starch digestibility of starchy foods: A review. *Food Chemistry, 406*, Article 135009. https://doi.org/10.1016/j.foodchem.2022.135009

Zambrano, Y., Contardo, I., Moreno, M. C., & Bouchon, P. (2022). Effect of extrusion temperature and feed moisture content on the microstructural properties of Rice-flour pellets and their impact on the expanded product. *Foods, 11*(2), 198. https://doi.org/10.3390/foods11020198

Zambrano, Y., Mariotti-Celis, M. S., & Bouchon, P. (2024). 3G extruded snacks enriched with catechin for high antioxidant capacity. *LWT - Food Science and Technology, 115674*. https://doi.org/10.1016/j.lwt.2023.115674

Zhang, H., Li, Z., Zhang, L., Lai, P. F., Tian, Y., Cui, S. W., & Ai, L. (2021). Effects of soluble dietary fibers on the viscosity property and digestion kinetics of corn starch digesta. *Food Chemistry, 338*, Article 127825. https://doi.org/10.1016/j.foodchem.2020.127825

Zhang, H., Sun, S., & Ai, L. (2022). Physical barrier effects of dietary fibers on lowering starch digestibility. *Current Opinion in Food Science, 48*, Article 100940. https://doi.org/10.1016/j.cofs.2022.100940

Zheng, J., Huang, S., Zhao, R., Wang, N., Kan, J., & Zhang, F. (2021). Effect of four viscous soluble dietary fibers on the physicochemical, structural properties, and in vitro digestibility of rice starch: A comparison study. *Food Chemistry, 130181*. https://doi.org/10.1016/j.foodchem.2021.130181

Zhou, Y., Dhital, S., Zhao, C., Ye, F., Chen, J., & Zhao, G. (2021). Dietary fiber-gluten protein interaction in wheat flour dough: Analysis, consequences and proposed mechanisms. *Food Hydrocolloids, 111*, Article 106203. https://doi.org/10.1016/j.foodhyd.2020.106203

Zhou, Z., Ye, F., Lei, L., Zhou, S., & Zhao, G. (2022). Fabricating low glycaemic index foods: Enlightened by the impacts of soluble dietary fiber on starch digestibility. *Trends in Food Science & Technology, 122*, 110–122. https://doi.org/10.1016/j.tifs.2022.02.016

Zhu, X. F., Tao, H., Wang, H. L., & Xu, X. M. (2023). Impact of water soluble arabinoxylan on starch-gluten interactions in dough. *LWT - Food Science and Technology, 173*, Article 114289. https://doi.org/10.1016/j.lwt.2022.114289